Anisotropic Heisenberg chain in coexisting transverse and longitudinal magnetic fields

D. V. Dmitriev* and V. Ya. Krivnov
Joint Institute of Chemical Physics of Russian Academy of Sciences, Kosygin Str.4, 117977, Moscow, Russia
(Received 2 March 2004; revised manuscript received 27 May 2004; published 25 October 2004)

The one-dimensional spin-1/2 *XXZ* model in a mixed transverse and longitudinal magnetic field is studied. Using the specially developed version of the mean-field approximation the order-disorder transition induced by the magnetic field is investigated. The ground-state phase diagram is obtained. The behavior of the model in the low transverse field is studied on the basis of conformal field theory. The relevance of our results to the observed phase transition in the quasi-one-dimensional antiferromagnet Cs_2CoCl_4 is discussed.

DOI: 10.1103/PhysRevB.70.144414 PACS number(s): 75.10.Jm

I. INTRODUCTION

The effects induced by magnetic fields in low-dimensional magnets are subjects of intensive theoretical and experimental research.[1–6] One of the striking effects is the dependence of magnetic properties of quasi-one-dimensional antiferromagnets with anisotropic exchange interactions on the direction of the applied magnetic field.[7–9] The basic model of such types of magnets is the anisotropic Heisenberg chain—the so-called *XXZ* model. It is, therefore, important to study the dependence of the properties of the *XXZ* chain on the field direction. There are two studied cases of the field direction. First is the *XXZ* model in the uniform longitudinal magnetic field. This model is exactly solved by the Bethe ansatz[10] and has been studied in great detail. In the second case the field is applied in the transverse direction. The *XXZ* model in the transverse field cannot be solved exactly and various approximate methods have been used for its study.[11–14] The behavior of the *XXZ* model in the symmetry-breaking transverse field is essentially different from the case of the longitudinal field. In particular, the transverse field induces the perpendicular antiferromagnetic long-range order (LRO) and the ground state quantum phase transition takes place at some critical field, where the LRO and the gap in the spectrum vanish. The phase transition of this type has been observed in the quasi-one-dimensional antiferromagnet Cs_2CoCl_4.[7] In fact, the magnetic field can have both longitudinal and transverse components. For example, the magnetic field in recent neutron scattering experiments on Cs_2CoCl_4 has been applied at an angle to the anisotropy axes. From this point, it is of particular interest to study the ground-state properties of the spin-$\frac{1}{2}$ *XXZ* chain in coexisting longitudinal H_z and transverse magnetic fields H_x. The Hamiltonian of this model is given by

$$H=\sum_{n=1}^{N}\left(S_n^xS_{n+1}^x+S_n^yS_{n+1}^y+\Delta S_n^zS_{n+1}^z\right)-h_z\sum_{n=1}^{N}S_n^z-h_x\sum_{n=1}^{N}S_n^x, \tag{1}$$

where

$$h_{x(z)}=\frac{g_{x(z)}\mu_B H_{x(z)}}{J} \tag{2}$$

is the effective dimensionless transverse (longitudinal) magnetic field, J is the exchange constant, and Δ is the anisotropy parameter, which is assumed to be $\Delta\geqslant -1$.

It was proposed[7] that low-energy properties of Cs_2CoCl_4 in the external magnetic field are described by the Hamiltonian (1) with $\Delta=0.25$ and $J=0.23$ meV. Evidently, in the case $\Delta=1$ the behavior of the system does not depend on the magnetic field direction and the model (1) reduces to the isotropic Heisenberg chain in a magnetic field $h=\sqrt{h_z^2+h_x^2}$. In the limiting case $\Delta\to\infty$ the model (1) reduces to the antiferromagnetic Ising chain in a mixed longitudinal and transverse field. This model was investigated in Refs. 15 and 16, where it was shown that there is a critical line in the (h_x,h_z) plane, where the ground state phase transition takes place. The critical behavior in the vicinity of this transition line belongs to the universality class of the two-dimensional Ising model.

Thus, the physics of the model (1) is very well understood in the case $h_x=0$ and is fairly good for the cases $h_z=0$ and $\Delta\to\infty$, but no detailed studies are available in general case. In this paper we study the model (1) using the mean-field approximation, which is the generalization of the approach developed in Ref. 13 for the case $h_z=0$. This method allows us to determine the transition line with high accuracy. The behavior in the low-h_x region will be considered using the conformal field theory method.

The paper is organized as follows. In Sec. II we consider a qualitative physical picture of the ground state phase diagram based on the classical approximation. In Sec. III the mean-field approach is developed and study of the critical properties of the model is presented. Scaling estimations of the gap and the LRO in low-h_x region are given in Sec. IV. The special case $\Delta=-1$ is studied in Sec. V. In Sec. VI we discuss our results in relation to the experimental data for Cs_2CoCl_4.

II. THE CLASSICAL APPROACH

In order to provide a physical picture of the phase diagram of the model (1) we use the classical approximation, when spins are represented as three-dimensional vectors. The variational wave function corresponding to the classical approximation has a form of a simple direct product of single-site spin states[17]

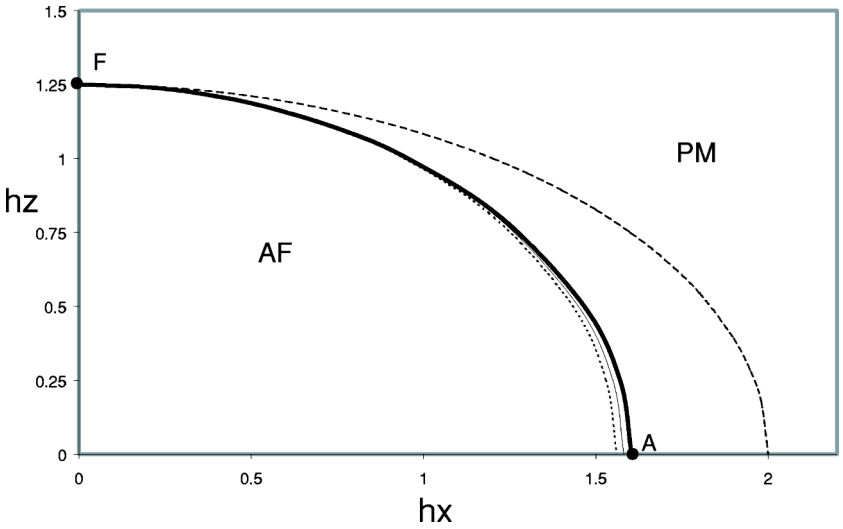

FIG. 1. The ground state phase diagram of the model (1) for $\Delta=0.25$. The transition line between the antiferromagnetic (AF) and paramagnetic (PM) states obtained in the mean-field approximation is shown by thick solid line and that in the classical approximation (9) by a dashed line. The thin solid line denotes the classical line (10) and dotted line corresponds to separatrix line (see Sec. III).

$$|\Phi_1\rangle = (1+A_1S_1^+)(1+A_2S_2^+)(1+A_1S_3^+)(1+A_2S_4^+)\cdots|\downarrow\downarrow\downarrow\cdots\rangle, \tag{3}$$

where A_1 and A_2 are variational parameters. If $A_1 \neq A_2$ then the ground state is twofold degenerate and another ground state wave function is

$$|\Phi_2\rangle = (1+A_2S_1^+)(1+A_1S_2^+)(1+A_2S_3^+)(1+A_1S_4^+)\cdots|\downarrow\downarrow\downarrow\cdots\rangle. \tag{4}$$

The form of the variational parameters A_1 and A_2 minimizing the energy is different in the regions $|\Delta|<1$ and $\Delta>1$. For the case $|\Delta|<1$ they can be chosen as[13]

$$A_1 = Ae^{i\phi}, \quad A_2 = Ae^{-i\phi}. \tag{5}$$

The ground state energy for this case calculated with Φ_1 (or Φ_2) is

$$\frac{E}{N} = \frac{A\cos 2\phi}{(1+A^2)^2} + \frac{\Delta(A^2-1)^2}{4(1+A^2)} - \frac{h_x A\cos\phi}{1+A^2} - \frac{h_z(A^2-1)}{1+A^2}. \tag{6}$$

Minimizing this energy over A and ϕ one obtains

$$\phi = \cos^{-1}\frac{h_x(\Delta+1)}{2\sqrt{(\Delta+1)^2-h_z^2}},$$

$$A = \sqrt{\frac{1+\Delta+h_z}{1+\Delta-h_z}}. \tag{7}$$

The twofold degenerate ground state at $\phi \neq 0$ is characterized by a nonzero staggered magnetization along the Y direction, which plays the role of the LRO parameter

$$\langle S_n^y\rangle = (-1)^n\frac{A\sin\phi}{1+A^2}. \tag{8}$$

For a given value of Δ the line of phase transition on (h_x,h_z) plane (the transition line) is determined by the condition $\phi=0$ and has a form

$$\frac{h_x^2}{4} + \frac{h_z^2}{(1+\Delta)^2} = 1. \tag{9}$$

This line separates the antiferromagnetic (AF) phase with the LRO from the paramagnetic (PM) phase with uniform magnetization. The transition line for $\Delta=0.25$ is shown on Fig. 1.

The case $\Delta>1$ can be analyzed in a similar way. In this case the twofold degenerate ground state in the AF phase is characterized by nonzero staggered magnetizations along the X and Z axes. But the expression for the transition line is rather cumbersome and we do not present it here. The transition line in the classical approximation for $\Delta=5$ is shown in Fig. 2.

As is well known[17] there is a remarkable, so-called "classical" or disorder line, which lies in the AF region in the (h_x,h_z) plane and is given by the equation

$$\frac{h_z^2}{(1+\Delta)^2} + \frac{h_x^2}{2(1+\Delta)} = 1. \tag{10}$$

The classical line is remarkable in a sense that the ground state on it is identical to the classical one and quantum fluctuations are missing. It was shown in Ref. 17 that the ground state of Eq. (1) on this line is twofold degenerate and the exact ground-state wave functions have the product form (3) and (4). The ground state energy on the classical line for any even N is

$$\frac{E}{N} = -\frac{1}{2} - \frac{\Delta}{4}. \tag{11}$$

From Eqs. (7) one can find that in the case $|\Delta|<1$ the magnetizations on the classical line are

$$\langle S_n^z\rangle = \frac{1}{2}\frac{h_z}{1+\Delta},$$

$$\langle S_n^x\rangle = \frac{h_x}{4},$$

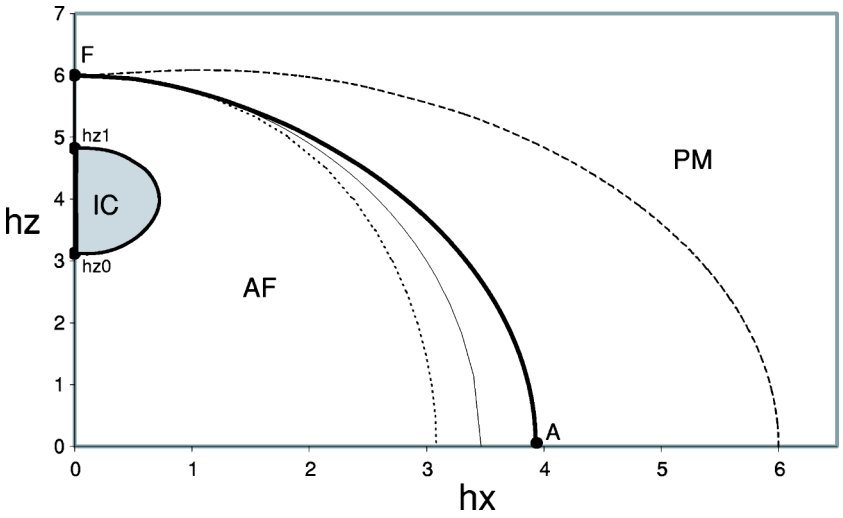

FIG. 2. The ground state phase diagram of the model (1) for $\Delta = 5$. The same notations as in Fig. 1 are used. The boundary of incommensurate critical (IC) phase is shown schematically (Sec. IV).

$$\langle S_n^y \rangle = (-1)^n \frac{h_x}{4} \sqrt{\frac{1-\Delta}{1+\Delta}}. \tag{12}$$

For $\Delta > 1$ the parameters A_1 and A_2 on the classical line are

$$A_{1,2} = \frac{1+\Delta+h_z}{h_x}\left(1 \pm \sqrt{\frac{\Delta-1}{\Delta+1}}\right), \tag{13}$$

and the magnetizations on two sublattices are

$$\langle S_n^x \rangle_{1,2} = \frac{A_{1,2}}{A_{1,2}^2+1},$$

$$\langle S_n^z \rangle_{1,2} = \frac{1}{2}\frac{A_{1,2}^2-1}{A_{1,2}^2+1},$$

$$\langle S_n^y \rangle_{1,2} = 0. \tag{14}$$

Thus, the classical approach shows that the ground state is different in the regions with $|\Delta| < 1$ and $\Delta > 1$. For $|\Delta| < 1$ the classical ground state is given by a configuration, with the spins on odd and even sites pointing, respectively, at angles χ and $-\chi$ with respect to the XZ plane. For $\Delta > 1$ in the ground state all spin vectors lie in the XZ plane with the spins on odd and even sites pointing, respectively, at angles φ_1 and φ_2 with respect to the X axis. This means that besides uniform magnetizations along X and Z axes in the AF region there is as well the staggered magnetizations: in the Y direction for $|\Delta| < 1$ and in both X and Z directions for $\Delta > 1$.[16] These facts are confirmed on the classical line, where the classical approximation gives the exact ground state.

Of course, one cannot expect that the classical approach gives an accurate estimation of the transition line and correct description of the phase transition (critical exponents).[13] Nevertheless, as it will be shown below, the fact of the generation of the staggered magnetizations in the Y direction for $|\Delta| < 1$ and in both the X and the Z directions for $\Delta > 1$ is qualitatively true.

III. MEAN-FIELD APPROXIMATION

Previously, the mean-field approximation (MFA) has been proposed to study the anisotropic Heisenberg chain in the transverse magnetic field.[13,14] It has been established that the MFA works very well if the transverse field is sufficiently strong and gives qualitative results for intermediate fields. For $\Delta > -0.5$ the MFA allows us to determine with high accuracy the critical transverse field at which the order-disorder transition occurs and to describe correctly the behavior of the system in the transition region. The MFA is based on the Jordan-Wigner transformation of spin-1/2 operators to the Fermi operators with the subsequent mean-field treatment of the Fermi Hamiltonian. In the case of coexisting transverse and longitudinal magnetic fields it is impossible to reduce the model Hamiltonian (1) to a local form in terms of the Fermi operators. Nevertheless, for this complicated case the MFA can be modified. In this section we develop the special version of the MFA, which remains the variational approach. This approach gives high accuracy in determining the transition line and correctly describes the whole ground state phase diagram.

At first we perform a rotation of the spins in the XZ plane by an angle φ:

$$S_n^x = \sigma_n^x \cos\varphi + \sigma_n^z \sin\varphi,$$

$$S_n^z = -\sigma_n^x \sin\varphi + \sigma_n^z \cos\varphi,$$

$$S_n^y = \sigma_n^y, \tag{15}$$

where σ_n^α are new spin-1/2 operators.

The Hamiltonian (1) is transformed to the form

$$H = \sum (x\sigma_n^x\sigma_{n+1}^x + \sigma_n^y\sigma_{n+1}^y + z\sigma_n^z\sigma_{n+1}^z) - h\sum \sigma_n^z + H',$$

$$H' = \frac{1-\Delta}{2}\sin 2\varphi \sum (\sigma_n^x\sigma_{n+1}^z + \sigma_n^z\sigma_{n+1}^x)$$

$$-(h_x\cos\varphi - h_z\sin\varphi)\sum \sigma_n^x, \tag{16}$$

where

$$x = \cos^2\varphi + \Delta\sin^2\varphi,$$

$$z = \Delta\cos^2\varphi + \sin^2\varphi,$$

$$h = h_z \cos\varphi + h_x \sin\varphi. \tag{17}$$

The angle φ is a variational parameter over which we will minimize the ground state energy.

After Jordan-Wigner transformation to the Fermi operators $a_n^\dagger$ and a_n

$$\sigma_n^\dagger = \exp\left(i\pi\sum_{j<n} a_j^\dagger a_j\right)a_n,$$

$$\sigma_n^z = \frac{1}{2} - a_n^\dagger a_n, \tag{18}$$

the Hamiltonian (16) takes the form

$$H_f = -\frac{hN}{2} + \frac{zN}{4} + \sum\left(h - z + \frac{1+x}{2}\cos k\right)a_k^\dagger a_k + \frac{1-x}{4}\sum \sin k(a_k^\dagger a_{-k}^\dagger + a_{-k}a_k) + z\sum a_n^\dagger a_n a_{n+1}^\dagger a_{n+1} + H_f'. \tag{19}$$

We treat the Hamiltonian H_f in the MFA, which implies the decoupling of the four-fermion term. The Fermi representation H_f' has a nonlocal form. But we note that all terms in H_f' contain an odd number of Fermi operators a_n and therefore $\langle H_f'\rangle = 0$ in the MFA. This fact holds the MFA in the frame of variational principle.

Thus, in the MFA the ground state energy E_0 and the one-particle excitation spectrum $\varepsilon(k)$ have the form:

$$E_0/N = -\frac{h}{2} + \frac{z}{4} + (h-z)\gamma_1 + \frac{1+x}{2}\gamma_2 + \frac{1-x}{4}\gamma_3 + z(\gamma_1^2 - \gamma_2^2 + \gamma_3^2), \tag{20}$$

$$\varepsilon(k) = \sqrt{(u + v\cos k)^2 + w^2\sin^2 k}, \tag{21}$$

where

$$u = h - z + 2z\gamma_1,$$

$$v = \frac{1+x}{2} - 2z\gamma_2,$$

$$w = \frac{1-x}{2} + 2z\gamma_3. \tag{22}$$

Quantities γ_1, γ_2, and γ_3 are the ground state expectation values, which are determined by the self-consistent equations:

$$\gamma_1 = \langle a_n^\dagger a_n\rangle = \int_0^\pi \frac{dk}{2\pi}\left(1 - \frac{u + v\cos k}{\varepsilon(k)}\right),$$

$$\gamma_2 = \langle a_n^\dagger a_{n+1}\rangle = -\int_0^\pi \frac{dk}{2\pi}\frac{(u + v\cos k)\cos k}{\varepsilon(k)},$$

$$\gamma_3 = \langle a_n^\dagger a_{n+1}^\dagger\rangle = -\int_0^\pi \frac{dk}{2\pi}\frac{w\sin^2 k}{\varepsilon(k)}. \tag{23}$$

The solution of the self-consistent equations (23) gives the minimum of the ground state energy (20) in a class of "one-particle" wave functions at a given angle φ. Thus, one should minimize the energy (20) with respect to the angle φ, solving the self-consistent equations (23) for each value of φ. This means that the proposed procedure remains the variational one.

The physical meaning of the angle φ is to show a direction of the total magnetization of the model (1),

$$S^z = \langle\sigma_n^z\rangle\cos\varphi = \left(\tfrac{1}{2} - \gamma_1\right)\cos\varphi,$$

$$S^x = \langle\sigma_n^z\rangle\sin\varphi = \left(\tfrac{1}{2} - \gamma_1\right)\sin\varphi. \tag{24}$$

Transforming the mean-field treated Fermi Hamiltonian back to the spin operators, we arrive at the well-studied anisotropic XY model in a longitudinal magnetic field,[18]

$$H_{XY} = \sum\left[(v-w)\sigma_n^x\sigma_{n+1}^x + (v+w)\sigma_n^y\sigma_{n+1}^y\right] - u\sum\sigma_n^z. \tag{25}$$

The model (25) has a transition line defined by the equation

$$u(h_x, h_z, \Delta) = v(h_x, h_z, \Delta), \tag{26}$$

which separates the region $u < v$ with the LRO represented by a staggered magnetization from the region $u > v$, where there is no LRO except for the uniform magnetization (24). The transition line $h_{zc}(h_x, \Delta)$ is determined by the numerical solution of Eqs. (23) and (26) with the minimization of the ground state energy over angle φ. The transition lines in the MFA for $\Delta = 0.25$ and $\Delta = 5$ are shown in Figs. 1 and 2 by thick solid lines.

It is well known[18] that the critical properties of the model (25) belong to the universality class of the two-dimensional Ising model. This means that in the MFA the gap is closed near the transition line linearly with the field and follows 1/8 law for the staggered magnetization.

The MFA also shows that for $|\Delta| < 1$ $(w > 0)$ the model has a staggered magnetization along the Y axis,

$$\langle(-1)^n S_n^y\rangle = \frac{[w^2(v^2 - u^2)]^{1/8}}{\sqrt{2(v+w)}}, \tag{27}$$

while for $\Delta > 1$ $(w < 0)$ the staggered magnetizations exist along the X and the Z axes:

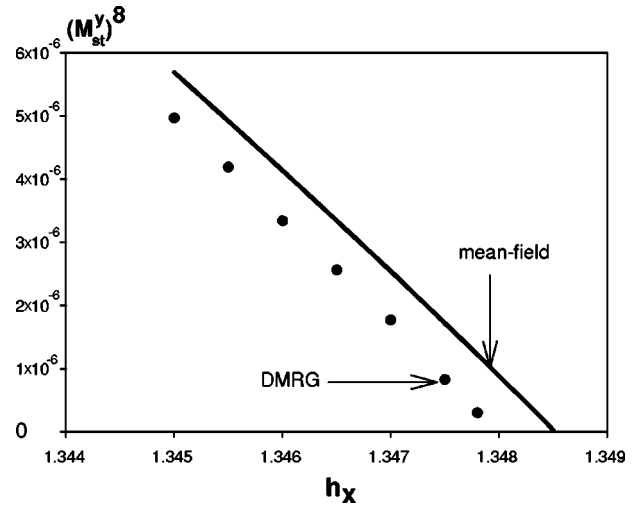

FIG. 3. The staggered magnetization near the transition line as a function of h_x for $\Delta=0.25$ and $h_z=0.67$.

$$\langle(-1)^n S_n^x\rangle = \frac{[w^2(v^2-u^2)]^{1/8}}{\sqrt{2(v-w)}}\cos\varphi,$$

$$\langle(-1)^n S_n^z\rangle = \frac{[w^2(v^2-u^2)]^{1/8}}{\sqrt{2(v-w)}}\sin\varphi. \tag{28}$$

The validity of the two-dimensional (2D) Ising type of the critical properties of the model (1) in the vicinity of the transition line has been checked by the density matrix renormalization group[19] (DMRG) calculations of the staggered magnetization and the gap. The staggered magnetization is computed as[14]

$$M_{st}^{\alpha} = \frac{1}{N}\langle 0|\sum(-1)^n S_n^{\alpha}|1\rangle, \quad \alpha=(x,y,z) \tag{29}$$

where $|0\rangle$ and $|1\rangle$ are two lowest-energy states. These states are degenerate (at $N\to\infty$) in the ordered AF phase. Therefore, in the AF phase the gap is given by the second excited state, while in the disordered PM phase the ground state is nondegenerate and the first excitation determines the gap in the spectrum. We have performed the DMRG calculations using the infinite-size algorithm and open boundary conditions and the number of states s kept in the DMRG truncating procedure is up to 25. We estimated the relative error due to DMRG truncation from difference between the data computed with $s=25$ and those with $s=20$ for chain lengths $N=202$. The estimated relative error is of the order of 10^{-5}, which is sufficiently small for accurate estimates for the gap and the staggered magnetization. As an example, in Figs. 3 and 4 we show the plots of $(M_{st}^y)^8$ and the gap m versus h_x in the vicinity of the transition point for $\Delta=0.25$ and fixed $h_z=0.67$ (these parameters are related to those for the antiferromagnet Cs_2CoCl_4). A good linearity of the plotted data definitely confirms the 2D Ising character of the transition line. The excellent agreement between the DMRG and the MFA results in Figs. 3 and 4 shows high accuracy of the MFA. For example, the critical field h_x estimated from the

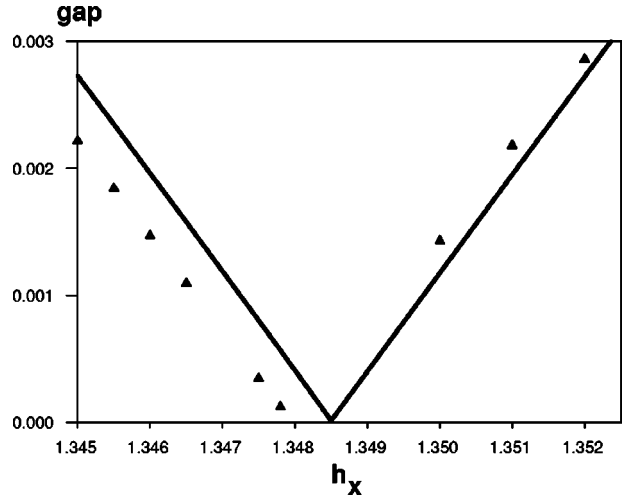

FIG. 4. The gap as a function of h_x near the transition line for $\Delta=0.25$ and $h_z=0.67$. (The solid line is the MFA, and triangles are DMRG results extrapolated to the thermodynamic limit.)

DMRG results differs from that obtained in the MFA within 0.04%.

In addition to the transition line defined by Eq. (26), the Hamiltonian (25) contains another special line defined by the equation

$$u^2+w^2=v^2. \tag{30}$$

This line separates the so-called "oscillatory" region $u^2+w^2<v^2$ (lying totally in the AF phase), where spin correlators of the model (25) have oscillatory behavior with an incommensurate wavelength depending on the model parameters (h_x,h_z,Δ), from the region without such oscillatory behavior of correlators.[18] The line (30) is nothing but the classical line of the model (1). Remarkably, the MFA gives the exact ground state on the classical line. Along this line the solution of Eqs. (23) has a simple form:

$$\sin^2\varphi = \frac{p}{1-p}\frac{1+\Delta}{1-\Delta}, \tag{31}$$

where

$$p = \frac{h_x^2}{4}\frac{1-\Delta}{1+\Delta}. \tag{32}$$

The values of γ_i for $|\Delta|<1$ are

$$\gamma_1 = \frac{1}{2}-\frac{\sqrt{1-p}}{2}, \quad \gamma_2=\gamma_3=-\frac{p}{4} \tag{33}$$

and for $\Delta>1$

$$\gamma_1 = \frac{1}{2}-\frac{1}{2\sqrt{1-p}}, \quad \gamma_2=-\gamma_3=\frac{p}{4(1-p)}. \tag{34}$$

The ground-state energy is given by Eq. (11). Substituting Eqs. (31)–(34) into Eqs. (24), (27), and (28), one can check that the magnetizations on the classical line in the MFA coincide with those given by Eqs. (12) and (14).

The gap on the classical line in the MFA lies at $k=\pi$ and equals

$$m = 1 - \frac{p}{2} - \sqrt{1-p}, \quad |\Delta| < 1$$

$$m = \left(1 - \frac{p}{2} - \sqrt{1-p}\right)\frac{1-2p-p\Delta}{(1-p)^2}, \quad \Delta > 1. \qquad (35)$$

It is necessary to note that the elementary excitation in the AF phase can be regarded as a domain wall between the two AF ground states. In the cyclic chain these excitations are created in pairs in contrast to open chains. In Eq. (19) the end-chain correction term is omitted, and the spectrum, Eq. (21), determines the gap for the open chain.[20,21] Therefore, in the AF region Eqs. (21) and (35) give half of the gap for a cyclic chain.

It is worth to mention one more special line on the phase diagram, so-called "separatrix," defined by the equation

$$uv = v^2 - w^2. \qquad (36)$$

This line separates the region $uv > v^2 - w^2$, where the lowest excitation has momentum $k_{min}=\pi$ from the region $uv < v^2 - w^2$ (situated entirely in the AF phase), where the lowest excitation has momentum, depending on the model parameters as

$$\cos k_{min} = \frac{uv}{w^2 - v^2}.$$

For any Δ, the transition line $h_{zc}(h_x,\Delta)$, the classical line $h_{zcl}(h_x,\Delta)$ and the separatrix $h_{zs}(h_x,\Delta)$ lie in the following sequence (see Figs. 1 and 2):

$$h_{zs}(h_x,\Delta) \leqslant h_{zcl}(h_x,\Delta) \leqslant h_{zc}(h_x,\Delta). \qquad (37)$$

All these lines meet each other only at point $F(h_x=0, h_z=1+\Delta)$.

A. Point *F*

Point $F(h_x=0, h_z=1+\Delta)$ is the special boundary point where all special lines terminate. The ground state at the point F is a saturated ferromagnet. Near point F ($h_x \ll 1$) the fermion density is small and the mean-field treatment of the four-fermion term in Eq. (19) gives an accuracy, at least, up to h_x^4. We omit intermediate calculations here and give the final expressions for the special lines. The transition and the separatrix lines near point F have the form:

$$h_{zc}(h_x,\Delta) = h_{zcl}(h_x,\Delta) + m_{cl} + O(h_x^6), \qquad (38)$$

$$h_{zs}(h_x,\Delta) = h_{zcl}(h_x,\Delta) - m_{cl} + O(h_x^6), \qquad (39)$$

where the behavior of the classical line $h_{zcl}(h_x,\Delta)$ is given by Eq. (10):

$$h_{zcl}(h_x,\Delta) = 1 + \Delta - \frac{h_x^2}{4} - \frac{h_x^4}{32(1+\Delta)} + O(h_x^6) \qquad (40)$$

and m_{cl} is the gap near point F on the classical line [see Eq. (35)]:

$$m_{cl} = \frac{h_x^4}{128}\left(\frac{1-\Delta}{1+\Delta}\right)^2 + O(h_x^6). \qquad (41)$$

As one can see the difference between three special lines near point F is very small, of the order of h_x^4.

The expressions for the gap are different to the left and to right of the separatrix line:

$$m = \frac{h_x^2}{4\sqrt{2}}\left|\frac{1-\Delta}{1+\Delta}\right|\sqrt{h_{zcl}(h_x,\Delta) - h_z}, \quad h_z < h_{zs}$$

$$m = |h_z - h_{zc}(h_x,\Delta)|, \quad h_z > h_{zs}. \qquad (42)$$

The linear behavior of the gap in the vicinity of the transition line confirms the 2D Ising universality class of the transition line.

The staggered magnetizations in the vicinity of point F vanish on two lines: on the transition line and on the line $h_x=0$. Equations (24), (27), and (28) near point F reduce to

$$\langle S_n^y \rangle = (-1)^n B,$$

$$B = \frac{1}{2}\left|\frac{1-\Delta}{1+\Delta}\right|^{1/4}\sqrt{h_x}\left(\frac{h_{zc}-h_z}{2}\right)^{1/8}, \qquad (43)$$

for $|\Delta| < 1$ and

$$\langle S_n^x \rangle = \frac{h_x}{4} + (-1)^n B,$$

$$\langle S_n^z \rangle = \frac{1}{2} - \frac{(-1)^n}{2} h_x B, \qquad (44)$$

for $\Delta > 1$. To validate our analysis in the vicinity of point F one should also estimate the effect of the part of the Hamiltonian H' in Eq. (16), omitted in the MFA. Near point F the angle $\varphi \approx h_x/2$ and, therefore, these terms in H' are small and can be taken into account as perturbations. The corresponding perturbation theory contains only even orders. The estimate of the second order shows that the contribution of these terms to the ground-state energy and to the gap is of the order of h_x^6 and $h_x^2(h_{zc}-h_z)$. This accuracy is sufficient to confirm the above equations. We note that in the limit $\Delta \to \infty$ point F transforms to the so-called multicritical point with a macroscopic degeneracy of the ground state.[22]

B. Point *A*

In the case $h_z=0$ the model (1) reduces to the anisotropic Heisenberg chain in the transverse magnetic field, which was studied in Refs. 11, 13, and 14. At some value of magnetic field $h_{xA}(\Delta)$ this model undergoes a transition from the antiferromagnetic state to the paramagnetic gapful state. We denote this transition by point A (see Figs. 1 and 2).

To study the behavior of the system in the vicinity of point A one can follow the arguments of Ref. 16, where point A was analyzed in detail for the special case $\Delta \to \infty$. As a result one finds that for $h_x = h_{xA}(\Delta)$ the perturbation theory in small parameter h_z contains infrared divergencies that are absorbed in a scaling parameter $y = h_z^2 N$. The analysis shows

that the mass gap generated by the longitudinal magnetic field h_z is proportional to h_z^2,

$$m = ah_z^2, \tag{45}$$

but the factor a is given not only by the second-order correction but also by all collected divergent orders of the perturbation series.

For a fixed value of Δ the behavior of the transition line in the (h_x, h_z) plane near point A can be found from the following consideration. As it was established above in the vicinity of the transition line the gap is proportional to the deviation from the line. This is valid for any direction of deviation except the direction at a tangent to the transition line. Thus, in the vicinity of point A on the line $h_x = h_{xA}(\Delta)$, the gap is

$$m \sim h_{xA}(\Delta) - h_{xc}(h_z, \Delta). \tag{46}$$

On the other hand, the gap is given by Eq. (45). Equalizing these two expressions for the gap we obtain the equation for the transition line in the vicinity of point A as

$$h_{xc}(h_z, \Delta) = h_{xA}(\Delta) - f(\Delta)h_z^2, \tag{47}$$

where the function $f(\Delta)$ is generally unknown and can be found numerically only.

Summarizing all above, we conclude that the MFA correctly describes the critical properties of the transition line and determines the transition line with high accuracy. This is because the MFA gives the exact ground state on the classical line, which is close to the transition line. In addition, the MFA is asymptotically exact in the vicinity of point F. Therefore, for any value of Δ, the accuracy in determining of the transition line drops as one moves from point F to point A. The MFA quality for the case $h_z = 0$ was investigated in Refs. 13 and 14, where it was shown that the accuracy of the MFA is high for $\Delta > -0.5$, and the MFA fails in the limit $\Delta \to -1$ (where the accuracy decreases to 20%). Besides, the high accuracy of the MFA in the vicinity of the transition line is confirmed by DMRG calculations (see Figs. 3 and 4). The MFA qualitative correctly describes the line $h_x = 0$ (no gap and soundlike spectrum for $h_z < 1 + \Delta$), but one cannot expect that the MFA gives correct critical exponents in low-h_x region.

IV. THE LOW-h_x REGION

On the line $h_x = 0$ the model (1) reduces to the well-known exactly solvable XXZ model in the longitudinal magnetic field. In this model three phases exist in different ranges of the magnetic field h_z: the ferromagnetic (F) phase at $h_z > 1 + \Delta$, the antiferromagnetic (AF) phase at $0 < h_z < h_{z0}(\Delta)$ [$h_{z0}(\Delta)$ is a lower critical field[23]], and the critical phase at $0 < h_z < 1 + \Delta$ ($|\Delta| < 1$) and $h_{z0}(\Delta) < h_z < 1 + \Delta$ ($\Delta > 1$).

In the F phase the ground state is a saturated ferromagnet $M \equiv \langle S_n^z \rangle = 1/2$ with a gap in the spectrum. In this region the appearance of the transverse magnetic field does not cause a noticeable change in the system properties. It results in the appearance of a uniform magnetization in the X direction and small decreasing of the magnetization in the Z direction.

In the AF region the system is in a gapful phase with the long-range Néel order M_{st}^z and zero uniform magnetization $M = 0$. Due to the gap in the spectrum the effect of the X component of magnetic field in the AF region can be obtained in the frame of a regular perturbation theory in h_x. The estimate of the first and the second orders in h_x indicates the appearance of the uniform magnetizations in both the X and the Z directions and the staggered magnetization in the X direction as

$$\langle S_n^x \rangle \sim h_x + (-1)^n h_z h_x,$$

$$\langle S_n^z \rangle \sim (-1)^n M_{st}^z + h_z h_x^2. \tag{48}$$

As follows from the last equations, in the case $h_z = 0$ the applied transverse magnetic field does not cause the uniform magnetization in the Z direction and the staggered magnetization in the X direction.[13]

The critical phase is characterized by nonzero magnetization $0 < M < 1/2$ in the ground state and by the massless spectrum. The low-energy properties in this phase are described by a free massless boson field theory with the Hamiltonian

$$H_0 = \frac{v}{2} \int dx [(\partial_x \Theta)^2 + (\partial_x \Phi)^2], \tag{49}$$

where $\Phi(x)$ and $\Theta(x)$ are the boson and dual field, respectively, and $v(\Delta, h_z)$ is the renormalized spin-wave velocity.

The spin-density operators are represented as[24]

$$S_n^z \simeq M + \frac{1}{2\pi R} \partial_x \Phi + a_1 (-1)^n \cos\left(\frac{\Phi}{R} + 2\pi M x \right),$$

$$S_n^x \simeq b_0 (-1)^n \cos(2\pi R \Theta) + b_1 \cos(2\pi R \Theta) \times \cos\left(\frac{\Phi}{R} + 2\pi M x \right), \tag{50}$$

where a_1, b_0, and b_1 are constants[25] and we identify the site index n with the continuous space variable x. The magnetization $M(\Delta, h_z)$ and the compactification radius $R(\Delta, M)$ are functions of Δ and h_z and can be determined by solving Bethe-ansatz integral equations.[26,27]

Both terms of operator S^x in Eq. (50) are oscillating when $M \neq 0$ and are not relevant to the uniform X component of the magnetic field. But as was shown in Ref. 28 the second term in Eq. (50) corresponding to perturbation

$$V_0 \sim h_x \cos(2\pi R \Theta) \cos\left(\frac{\Phi}{R} + 2\pi M x \right) \tag{51}$$

has conformal spin $S = 1$ and generates two other perturbations with zero conformal spin:

$$V_1 \sim h_x^2 \cos(4\pi R \Theta),$$

$$V_2 \sim h_x^2 \cos\left(\frac{2\Phi}{R} + 4\pi M x \right). \tag{52}$$

The scaling dimensions of perturbations V_1 and V_2 are 2η and $2/\eta$ ($\eta = 2\pi R^2$), respectively. The perturbation V_2 describes umklapp processes and it is responsible for the gap generation in the AF region, where $M = 0$. But in the critical

region ($h_z > 0$) the magnetization $M \neq 0$ and the perturbation V_2 as well as the operator V_0 does not conserve the total momentum and will be frozen out.

Therefore, in the uniform longitudinal magnetic field h_z the critical exponent for the mass gap is determined by the only nonoscillating perturbation V_1:

$$m \sim h_x^{1/(1-\eta)}. \tag{53}$$

We note that in the special case $h_z = 0$ ($|\Delta| < 1$) the magnetization $M = 0$ and all perturbations V_0, V_1, and V_2 are nonoscillating.[29] In this case in the region $\Delta > \cos[\pi\sqrt{2}] \approx -0.266$ the perturbation V_0 becomes most relevant and determines the mass gap as[13]

$$m \sim h_x^{2/(4-\eta-1/\eta)}. \tag{54}$$

The perturbation V_1 corresponds to the spin-nonconserving operator $\Sigma(S_n^x S_{n+1}^x - S_n^y S_{n+1}^y)$.[24] This means that the behavior of the system (1) at small h_x is similar to that of well studied XYZ chain in magnetic field h_z with small anisotropy in the XY plane.[30] Using the results of Ref. 30 we conclude that in the region $\Delta > 1$ the presence of a small X component of magnetic field leads to a sequence of three transitions with increasing longitudinal magnetic field h_z. The first one occurs at $h_{z0}(\Delta)$ ($\eta = 2$), where the AF phase transforms to the incommensurate critical (IC) or "floating" phase (see Fig. 2). In the IC phase the perturbation V_1 is irrelevant and the spectrum remains gapless. Here the correlation functions display a power-law decay with a magnetization dependent wave vector. There is no LRO in the IC phase, except uniform magnetizations M and $\langle S_n^x \rangle = \chi_x h_x$ (the susceptibility χ_x is finite in the critical phase). Unfortunately, neither the field theory approach nor the MFA allows us to determine the boundary of the IC phase. Therefore, this phase boundary is shown on Fig. 2 schematically.

Further increasing of h_z leads to the transition of the Kosterlitz-Thouless type taking place at the point $h_{z1}(\Delta)$ where $\eta = 1$. At $h_z > h_{z1}(\Delta)$ the perturbation V_1 becomes relevant ($\eta < 1$) and the system crosses from the IC phase to a strong-coupling regime with the staggered magnetizations in both X and Z directions (AF phase).

The last transition with further increasing of h_z occurs near the point F at $h_z = h_{zc}$ (see Fig. 2). This transition to the PM phase was studied in Sec. III.

The field theory approach allows us also to determine the exponent for the LRO. The transverse magnetic field generates the staggered magnetization along the Y axis at $|\Delta| < 1$ as

$$\langle S_n^y \rangle \sim \frac{(-1)^n}{\xi^{\eta/2}} \sim (-1)^n m^{\eta/2} \sim (-1)^n h_x^{\eta/(2-2\eta)} \tag{55}$$

and along X and Z axes at $\Delta > 1$ and $h_{z1}(\Delta) < h_z < 1 + \Delta$,

$$\langle S_n^x \rangle \sim \chi_x h_x + (-1)^n h_x^{\eta/(2-2\eta)},$$

$$\langle S_n^z \rangle \sim M + (-1)^n h_x^{(2-\eta)/(2-2\eta)}. \tag{56}$$

We note, that in the limit $h_z \to 1 + \Delta$ ($\eta \to 1/2$), the exponents for the mass gap (53) and staggered magnetizations in Eqs. (55) and (56) agree with the MFA results in Eqs. (42)–(44).

The staggered magnetization along the Z axis in Eq. (56) can be derived in the same manner as was derived the generated perturbations V_1 and V_2 in Eqs. (52). According to Eqs. (50) the nonzero contribution to the first-order correction in h_x to the staggered magnetization $\langle (-1)^n S_n^z \rangle$ is given by the following terms in spin-density operators:

$$(-1)^n S_n^z \sim \cos\left(\frac{\Phi}{R} + 2\pi M x\right),$$

$$S_n^x \sim \cos(2\pi R\Theta)\cos\left(\frac{\Phi}{R} + 2\pi M x\right). \tag{57}$$

Then the leading contribution comes from small distances of order of ultraviolet cutoff (the lattice constant)

$$\begin{aligned}(-1)^{x_1} S^z(z_1) &\sim h_x \int d^2 z_2 e^{i2\pi M(x_2 - x_1)} \exp\left[-i\frac{\Phi(z_1)}{R}\right] \\ &\times \exp\left[i\frac{\Phi(z_2)}{R}\right] \cos[2\pi R\Theta(z_2)] \\ &\sim h_x \cos[2\pi R\Theta(z_1)] \sim h_x (-1)^{x_1} S^x(z_1).\end{aligned} \tag{58}$$

Thus, the relation between the staggered magnetization along X and Z axes is established,

$$\langle (-1)^n S_n^z \rangle \sim h_x \langle (-1)^n S_n^x \rangle, \tag{59}$$

which results in the critical exponent for $\langle (-1)^n S_n^z \rangle$ written in Eq. (56).

V. SPECIAL CASE $\Delta = -1$

When $\Delta \to -1$ point F tends to zero, and exactly on the line $\Delta = -1$ both classical and transition lines disappear. In the vicinity of the line $\Delta = -1$ it is convenient to rotate the coordinate system in such a way that the Hamiltonian (1) takes the form

$$H = H_0 + V_h + V_\Delta,$$

$$H_0 = -\sum \mathbf{S}_n \cdot \mathbf{S}_{n+1} - h_x \sum (-1)^n S_n^z,$$

$$V_h = -h_z \sum S_n^x,$$

$$V_\Delta = (1 + \Delta) \sum S_n^x S_{n+1}^x. \tag{60}$$

The unperturbed Hamiltonian H_0 describes the critical behavior of the system at $0 < h_x < h_0$,[31] where the estimate of h_0 is $h_0 \approx 0.53(3)$.[13] The spin-density operators of H_0 are related to the bosonic fields by Eqs. (50) with $M = 0$, where the compactification radius $R(h_x)$ is a function of h_x. This dependence is generally unknown, but the limiting values of $\eta(h_x) = 2\pi R^2(h_x)$ are known:[13]

$$\eta(h_x) = \frac{h_x}{\pi}, \quad h_x \to 0$$

$$\eta(h_x) = \frac{1}{4}, \quad h_x \to h_0. \tag{61}$$

The perturbations V_h and V_Δ have scaling dimensions $\eta/2$ and 2η, respectively. Therefore, according to Eqs. (61) both perturbations V_h and V_Δ are relevant in the critical region $0<h_x<h_0$ and produce mass gaps

$$m_h \sim h_z^{1/(2-\eta/2)},$$

$$m_\Delta \sim |1+\Delta|^{1/(2-2\eta)}. \tag{62}$$

In particular, $m_h \sim \sqrt{h_z}, m_\Delta \sim \sqrt{|1+\Delta|}$ at $h_x \to 0$ and $m_h \sim h_z^{8/15}, m_\Delta \sim |1+\Delta|^{2/3}$ at $h_x \to h_0$.

The gap at $\Delta=-1$ and for $h_x, h_z \ll 1$ can be asymptotically exactly described by the spin-wave theory.[13] The validity of the spin-wave approximation is quite natural because the number of magnons forming the ground state is small for $h_x, h_z \ll 1$. The spin-wave result for the gap is

$$m = \sqrt{h_z(h_z + h_x^2/2)}. \tag{63}$$

For $h_z \ll h_x^2 \ll 1$ Eq. (63) agrees with the conformal theory result, Eq. (62), at $\eta \to 0$ and gives the preexponential factor for the gap.

VI. DISCUSSION AND CONCLUSION

As mentioned earlier the order-disorder transition induced by the magnetic field has been observed in the quasi-one-dimensional antiferromagnet Cs_2CoCl_4 described, as supposed, by the model (1) with $\Delta=0.25$. It is interesting to compare the magnetization curves obtained in the neutron-scattering experiment[7] with those in the MFA. In this experiment the magnetic field H has been applied at an angle $\beta \simeq 40°$ to the XY plane. This means that $H_x \simeq H_z \simeq H/\sqrt{2}$. According to Ref. 7, g factors in Cs_2CoCl_4 are $g_{x,y}=2g_z=4.80$. Therefore, the ratio of the effective fields in the model (1) is $h_x/h_z=2H_x/H_z \simeq 2$. The total magnetization M_{tot} is

$$M_{tot} = \frac{\mu_B}{\sqrt{2}}(g_x\langle S_n^x\rangle + g_z\langle S_n^z\rangle), \tag{64}$$

where $\langle S_n^x\rangle$ and $\langle S_n^z\rangle$ are the magnetizations calculated in the MFA at the effective fields $h_x=2h_z$. The AF ordered moment is given by $M_{st}=g_y\mu_B\langle|(-1)^n S_n^y|\rangle$. In Fig. 5 we plot M_{tot} and M_{st} as the functions of the magnetic field H ($H=\sqrt{2}h_xJ/g_x\mu_B$). These magnetization curves are qualitative similar to the experimental ones (Figs. 12 and 14 in Ref. 7). The maximal value of staggered magnetization $1.7\mu_B$ agrees with the experimental magnitude of the AF ordered moment $1.6\mu_B$. The total magnetization at $H \to \infty$ in the MFA $M_{tot}=1.9\mu_B$ is consistent with the saturation moment $1.7\mu_B$ estimated in Ref. 7. At the same time, there is an essential difference in the low-field behavior of M_{st}. The experimental AF ordered moment is finite at $H=0$, while $M_{st}=0$ at $H=0$ in Fig. 5. This difference is due to weak interchain couplings, which form the magnetically ordered ground state in the real compound at $H=0$, and this effect is absent in the one-dimensional model (1). The behavior of the magnetizations in the vicinity of the critical field in Fig. 5 is similar to the experimental curve. But the value of the critical field on Fig. 5 is 1.6 T, while the experimental value is 2.1 T. We do not believe that the MFA is the reason for this discrepancy. The possible reason may lie in the fact that Cs_2CoCl_4 is described by the $s=\frac{3}{2}$ antiferromagnetic model with strong single-ion anisotropy and its reducing to the $s=\frac{1}{2}$ model is approximate.

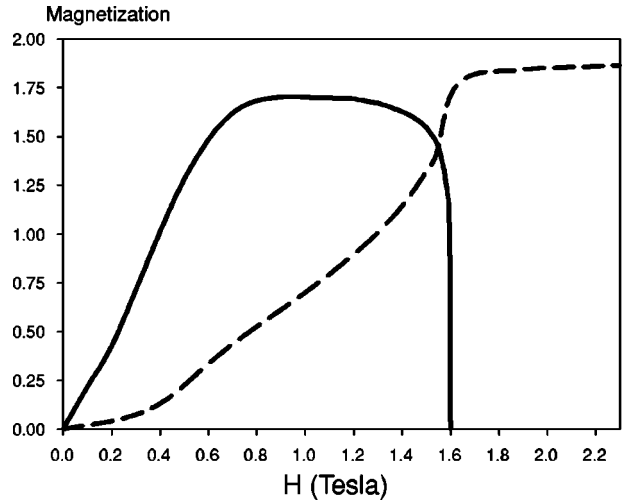

FIG. 5. Uniform (dashed line) and staggered (solid line) magnetization curves.

Magnetic measurements in Ref. 7 were performed in the field applied at a fixed angle β to the anisotropy axis. It is interesting to consider how the properties of the model (1) are changed when the magnetic field is turned from purely longitudinal ($\beta=0$) to the transverse direction ($\beta=\pi/2$). If the effective field h is in the range $(1+\Delta)<h<h_{xA}(\Delta)$ for $|\Delta|<1$ or $h_{xA}(\Delta)<h<(1+\Delta)$ for $\Delta>1$ then there is the critical angle β_0, which is defined by the intersection of the circle $h_x^2+h_z^2=h^2$ with the transition line. At this angle the phase transition from the AF phase at $\beta>\beta_0$ ($\beta<\beta_0$) for $\Delta<1$ ($\Delta>1$) to the PM phase at $\beta<\beta_0$ ($\beta>\beta_0$) takes place. The staggered magnetization and the gap vanish at $\beta=\beta_0$ as $M_{st} \sim |\beta-\beta_0|^{1/8}$ and $m \sim |\beta-\beta_0|$.

In conclusion, we have studied the spin-$\frac{1}{2}$ XXZ Heisenberg chain in the mixed longitudinal and transverse magnetic field. It was shown that the ground-state phase diagram on the (h_x, h_z) plane contains the AF and the PM phases separated by the transition line. The transition line was determined using the proposed special version of the MFA, which reduces the XXZ model in the mixed fields to the XY model in the uniform longitudinal field. The MFA gives the transition line with high accuracy at least for $\Delta \geqslant -0.5$. This fact is confirmed by comparison of the MFA results with DMRG calculations. The MFA gives a satisfactory description of the whole phase diagram, though the critical exponents of low-h_x dependence of the gap and the magnetization cannot be found correctly in the MFA. These exponents have been found with use of the conformal field method.

The field theory approach also shows that in the region $\Delta > 1$ the phase diagram contains IC or floating phase characterized by the gapless spectrum and power-law decay of correlation functions. The form of the boundary of IC phase can be determined only numerically. But this boundary is located certainly on the left of the classical line, where the spectrum is gapped.

We believe that the modified MFA is suitable for the studying of the magnetic phase transitions of the quasi-one-dimensional anisotropic magnets induced by the applied magnetic field. The important problem is to take into account effects of interchain interactions.[32]

ACKNOWLEDGMENTS

We thank Dr. V. Cheranovskii for useful discussions. This work was supported under RFBR Grant No. 03-03-32141 and ISTC No. 2207.

*Electronic address: dmitriev@deom.chph.ras.ru

[1] D. C. Dender, P. R. Hammar, D. H. Reich, C. Broholm, and G. Aeppli, Phys. Rev. Lett. **79**, 1750 (1997).
[2] R. Helfrich, M. Koppen, M. Lang, F. Steglich, and A. Ochiku, J. Magn. Magn. Mater. **177**, 309 (1998).
[3] M. Kohgi, K. Iwasa, J.-M. Mignot, B. Fåk, P. Gegenwart, M. Lang, A. Ochiai, H. Aoki, and T. Suzuki, Phys. Rev. Lett. **86**, 2439 (2001).
[4] I. Affleck and M. Oshikawa, Phys. Rev. B **60**, 1038 (1999).
[5] J. Lou, S. Qin, C. Chen, Z. Su, and L. Yu, Phys. Rev. B **65**, 064420 (2002).
[6] F. H. L. Essler, A. Furusaki, and T. Hikihara, Phys. Rev. B **68**, 064410 (2003).
[7] M. Kenzelmann, R. Coldea, D. A. Tennant, D. Visser, M. Hofmann, P. Smeibidl, and Z. Tylczynski, Phys. Rev. B **65**, 144432 (2002).
[8] G. Uimin, Y. Kudasov, P. Fulde, and A. A. Ovchinnikov, Eur. Phys. J. B **16**, 241 (2000).
[9] A. Dutta, D. Sen, Phys. Rev. B **67**, 094435 (2002).
[10] C. N. Yang and C. P. Yang, Phys. Rev. **150**, 321 (1966); **150**, 327 (1966).
[11] S. Mori, J.-J. Kim, and I. Harada, J. Phys. Soc. Jpn. **64**, 3409 (1995).
[12] Y. Hieida, K. Okunishi, and Y. Akutsu, Phys. Rev. B **64**, 224422 (2001).
[13] D. V. Dmitriev, V. Ya. Krivnov, A. A. Ovchinnikov, and A. Langari, Zh. Eksp. Teor. Fiz. **122**, 624 (2002) [JETP **95**, 538 (2002)]; D. V. Dmitriev, V. Ya. Krivnov, and A. A. Ovchinnikov, Phys. Rev. B **65**, 172409 (2002).
[14] J.-S. Caux, F. H. L. Essler, and U. Low, Phys. Rev. B **68**, 134431 (2003).
[15] P. Sen, Phys. Rev. E **63**, 016112 (2001).
[16] A. A. Ovchinnikov, D. V. Dmitriev, V. Ya. Krivnov, and V. O. Cheranovskii, Phys. Rev. B **68**, 214406 (2003).
[17] J. Kurmann, H. Tomas, and G. Muller, Physica A **112**, 235 (1982); G. Muller and R. E. Shrock, Phys. Rev. B **32**, 5845 (1985).
[18] E. Barouch and B. M. McCoy, Phys. Rev. A **3**, 786 (1971).
[19] S. R. White, Phys. Rev. B **48**, 10 345 (1993).
[20] E. Lieb, T. Schultz, and D. Mattis, Ann. Phys. (N.Y.) **16**, 407 (1961).
[21] P. Pfeuty, Ann. Phys. (N.Y.) **57**, 79 (1970).
[22] C. Domb, Adv. Phys. **9**, 149 (1960).
[23] J. des Cloizeaux and M. Gaudin, J. Math. Phys. **7**, 1384 (1966).
[24] A. O. Gogolin, A. A. Nersesyan, and A. M. Tsvelik, *Bosonization and Strongly Correlated Systems* (Cambridge University Press, Cambridge, 1998).
[25] T. Hikihara and A. Furusaki, Phys. Rev. B **69**, 064427 (2004).
[26] N. M. Bogoliubov, A. G. Izergin, and V. E. Korepin, Nucl. Phys. B **275**, 687 (1986).
[27] D. C. Cabra, A. Honecker, and P. Pujol, Phys. Rev. B **58**, 6241 (1998).
[28] A. A. Nersesyan, A. Luther, and F. V. Kusmartsev, Phys. Lett. A **176**, 363 (1993).
[29] M. Bocquet, F. H. L. Essler, A. M. Tsvelik, and A. O. Gogolin, Phys. Rev. B **64**, 094425 (2001).
[30] T. Giamarchi and H. J. Schulz, J. Phys. (Paris) **49**, 819 (1988).
[31] F. C. Alcaraz and A. L. Malvezzi, J. Phys. A **28**, 1521 (1995); M. Tsukano and K. Nomura, J. Phys. Soc. Jpn. **67**, 302 (1998).
[32] D. V. Dmitriev and V. Ya. Krivnov, Pis'ma Zh. Eksp. Teor. Fiz. **80**, 349 (2004) [JETP Lett. **80**, 303 (2004)].